Critically Sampled Composite Wavelets

Glenn R. Easley
System Planning Corporation,
3601 Wilson Blvd
Arlington, VA 22201 USA

Demetrio Labate
Department of Mathematics,
University of Houston,
Houston, TX 77204 USA

***Abstract*—Wavelets with composite dilations were introduced to provide a framework for the construction of waveforms defined not only at various scales and locations but also at various orientations. The shearlet system, which provides optimally sparse representations of images with edges, is a particular well-known example of these systems. In this work, we develop critically sampled wavelet transforms with composite dilations for the purpose of image coding. We show that these new critically sampled transforms can achieve much better non-linear approximation rates for images containing edges than traditional discrete wavelet transforms or even more sophisticated multiscale transforms such as the critically sampled contourlet transform.**

***Index Terms*—** wavelets, shearlets

I. Introduction

Despite their spectacular success in signal and image processing applications, it is now generally acknowledged that traditional wavelets are not particularly efficient in dealing with multidimensional data, due to their limited ability to process geometric information. In response to this limitation, several methods have been introduced in recent years in computational harmonic analysis, most notably the curvelets and shearlets, which offer optimally sparse representations of images with edges [1], [2]. While both representations provide a directional multiscale decomposition of images, the shearlets, which are a special realization of the theory of *wavelets with composite dilations*, offer the additional advantage of being based on the framework of affine systems. This enables a natural transition from the continuous to the discrete setting and a greater flexibility in the development of discrete directional multiscale schemes.

In the drive to develop more geometrically oriented transforms that are critically sampled, new variations of the contourlet transform have also been made [3], [4], [5]. In this work, we construct critically sampled transforms that are examples of or are related to the theory of wavelets with composite dilations. Similar constructions such as those provided [6], [7], [8], [3] can also be viewed as closely related to examples of our general framework.

A. Wavelets with composite dilations

For $y \in \mathbb{R}^n$, the *translation operator* T_y is defined by

$$T_y\, f(x) = f(x-y).$$

For $a \in GL_n(\mathbb{R})$ the *dilation operator* D_a is defined by

$$D_a\, f(x) = |\det a|^{-1/2}\, f(a^{-1}x).$$

The *affine* or *wavelet systems* generated by $\Psi = \{\psi_1, \dots, \psi_L\} \subset L^2(\mathbb{R}^n)$ and $A = \{a^i : i \in \mathbb{Z}\}$, are the systems of the form

$$\mathcal{A}_A(\Psi) = \{D_a\, T_k\, \psi_m : a \in A,\, m = 1, \dots, L\}.$$

If $\mathcal{A}_A(\Psi)$ is a Parseval frame for $L^2(\mathbb{R}^n)$, then Ψ is called a *multiwavelet* or, simply, a *wavelet* if $\Psi = \{\psi\}$. If, in addition, $\mathcal{A}_A(\Psi)$ is an orthonormal basis, then Ψ is an orthonormal (multi)wavelet.

By extending this idea, one introduces the *affine systems with composite dilations*, which have the form

$$\mathcal{A}_{AB}(\Psi) = \{D_a D_b\, T_k\, \Psi : k \in \mathbb{Z}^n,\, a \in A,\, b \in B\},$$

where $A,\, B \subset GL_n(\mathbb{R})$. If $\mathcal{A}_{AB}(\Psi)$ is a Parseval frame (orthonormal basis), then Ψ will be called a *composite* or *AB-multiwavelet* (orthonormal composite wavelet). The theory of these systems generalizes the classical theory of wavelets and provides a simple and flexible framework for the construction of Parseval frames and orthonormal bases that exhibit a number of geometric features of great potential in applications. In fact, the matrices $a \in A$ are expanding matrices and are associated with the usual multiscale decomposition; the matrices $b \in B$, on the other hand, are non-expanding and are associated with rotations and other orthogonal transformations. As a result, one can construct composite wavelets with good time-frequency decay properties whose elements contain "long and narrow" waveforms with many locations, scales, shapes and directions.

II. Novel Constructions

The theory of wavelets with composite dilations extends many of the standard results of the classical wavelet theory. We refer to [9], [10], [11] for a detailed description of this theory. For the constructions considered in this paper, it will be sufficient to recall the following results from [10], which provides relatively simple conditions for the constructions of composite wavelets of the form $\psi = (\chi_S)^\vee$, where $S \subset \mathbb{R}^2$.

Theorem 1: Let $\psi = (\chi_S)^\vee$ and suppose that $S \subset F \subset \mathbb{R}^2$, where

1) $\widehat{\mathbb{R}}^2 = \bigcup_{k \in \mathbb{Z}^2} (F + k)$;
2) $\widehat{\mathbb{R}}^2 = \bigcup_{c \in \mathcal{C}} S\, c^{-1}$,

where the union is essentially disjoint and $\mathcal{C}$ is a subset of $GL_2(\mathbb{R})$. Then the system $\mathcal{A}_{\mathcal{C}}$ is a Parseval frame for $L^2(\mathbb{R}^2)$.

Indeed, using Theorem 1, we obtain the following constructions which provide the framework for novel discrete directional multiscale systems.

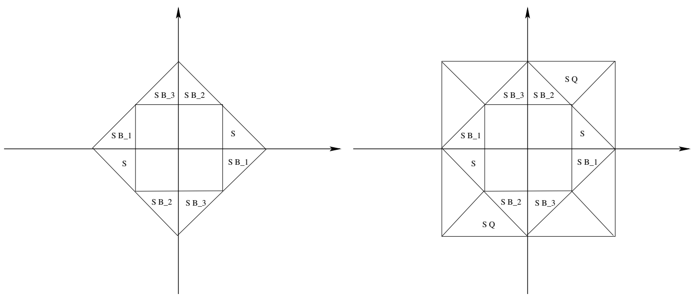

Fig. 1. *Example of composite wavelet where $a = Q$.*

A. Example 1

Let $a = Q = \begin{pmatrix} 1 & 1 \\ -1 & 1 \end{pmatrix}$ and consider $B = \{b_0, b_1, b_2, b_3\}$ where $b_0 = \begin{pmatrix} 1 & 0 \\ 0 & 1 \end{pmatrix}$, $b_1 = \begin{pmatrix} 1 & 0 \\ 0 & -1 \end{pmatrix}$, $b_2 = \begin{pmatrix} 0 & 1 \\ 1 & 0 \end{pmatrix}$, $b_3 = \begin{pmatrix} 0 & -1 \\ -1 & 0 \end{pmatrix}$.

Let $\hat{\psi}(\xi) = \chi_S(\xi)$ where the set S is the union of the triangles with vertices $(1,0),(2,0),(1,1)$ and $(-1,0),(-2,0),(-1,-1)$ and is illustrated in Figure 1. Notice that S satisfies the assumptions of Theorem 1. Hence the system

$$\{D_a^i\, D_b\, T_k\, \psi : \, i \in \mathbb{Z}, \, b \in B, \, k \in \mathbb{Z}^2, \}$$

is an ONB for $L^2(\mathbb{R}^2)$ (since it is a PF and, in addition, $\|\psi\| = 1$).

Indeed, a construction in [8] is a modification of this one which is obtained by splitting each triangle of the set S into 2 smaller triangles, say, $S = S_1 \cup S_1$, so that we have the frequency tiling illustrated in Figure 2. This can be expressed as the composite wavelet system

$$\{D_a^i\, D_b\, T_k\, \psi^m : \, i \in \mathbb{Z}, \, b \in B, \, k \in \mathbb{Z}^2, m = 1,2\},$$

where $\hat{\psi}^m(\xi) = \chi_{S_m}(\xi)$, $m = 1,2$.

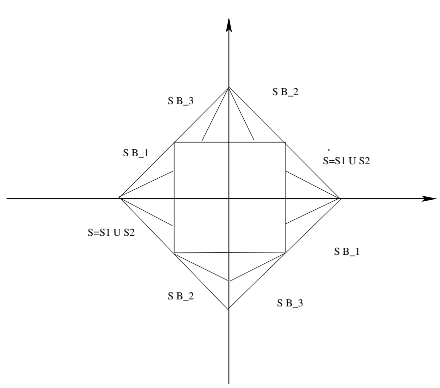

Fig. 2. *Example of composite wavelet system with $a = Q$.*

B. Example 2

Let $a = \begin{pmatrix} 2 & 0 \\ 0 & 2 \end{pmatrix}$ and consider $B = \{b, b_1, b_2, b_3\}$ where $b_0 = \begin{pmatrix} 1 & 0 \\ 0 & 1 \end{pmatrix}$, $b_1 = \begin{pmatrix} 1 & 0 \\ 0 & -1 \end{pmatrix}$, $b_2 = \begin{pmatrix} 0 & 1 \\ 1 & 0 \end{pmatrix}$, $b_3 = \begin{pmatrix} 0 & -1 \\ -1 & 0 \end{pmatrix}$.

Let R be the union of the trapezoid with vertices $(1,0),(2,0),(1,1),(2,2)$ and the symmetric one with vertices $(-1,0),(-2,0),(-1,-1),(-2,-2)$. Next, we partition each trapezoid into equilateral triangles R_m, $m = 1,2,3$ as illustrated in Figure 3. Hence we define $\hat{\psi}^m(\xi) = \chi_{R_m}(\xi)$, $m = 1,2,3$. Then the system

$$\{D_a^i\, D_b\, T_k\, \psi^m : \, i \in \mathbb{Z}, \, b \in B, \, k \in \mathbb{Z}^2, m = 1,2,3\}$$

is an orthonormal basis for $L^2(\mathbb{R}^2)$.

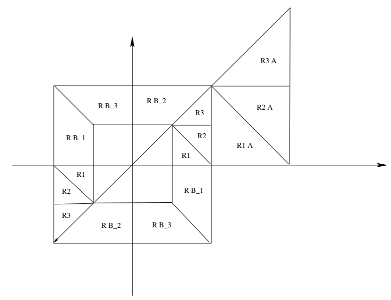

Fig. 3. *Example of composite wavelet system with $a = 2I$.*

C. Example 3

An interesting variant of the system described above is obtained by keeping the same dilation matrix a and replacing B with the set $B = \{b^\ell : -3 \le \ell \le 2\}$ where b is the shear matrix $\begin{pmatrix} 1 & 1 \\ 0 & 1 \end{pmatrix}$. Then, by letting R be the union of the trapezoid with vertices $(1,0),(2,0),(1,1/3),(2,2/3)$ and the symmetric one with vertices $(-1,0),(-2,0),(-1,-1/3),(-2,-2/3)$, and $\hat{\psi}^m(\xi) = \chi_{R_m}(\xi)$, where $R_m = R\, b^m$, it follows that the system

$$\{D_a^i\, D_b\, T_k\, \psi^m : \, i \in \mathbb{Z}, \, b \in B, \, k \in \mathbb{Z}^2, m = 1,2,3\}$$

is an orthonormal basis for $L^2(\mathcal{D}_0) = \{f \in L^2(\mathbb{R}^2) : \operatorname{supp} \hat{f} \subset \mathcal{D}_0\}$, where $\mathcal{D}_0 = \{(\omega_1, \omega_2) : |\omega_2/\omega_1| \le 1\}$. To obtain an orthonormal basis for the whole space $L^2(\mathbb{R}^2)$, it is sufficient to add another system, similar to the one above, which is an orthonormal basis for $L^2(\mathcal{D}_1)$ where $\mathcal{D}_1 = \{(\omega_1, \omega_2) : |\omega_2/\omega_1| \ge 1\}$. This is simply obtained as

$$\{D_a^i\, D_b\, T_k\, \tilde{\psi}^m : \, i \in \mathbb{Z}, \, b \in \tilde{B}, \, k \in \mathbb{Z}^2, m = 1,2,3\},$$

where $B = \{(b^T)^\ell : -3 \le \ell \le 2\}$.

Notice that, for this example, as well as for other examples of composite wavelets, it is possible to modify the construction in such a way that $\hat{\psi}$ is a smooth function and not the characteristic function of a set. The last construction, in particular, is related to the *shearlet system*, a Parseval frame of well-localized waveforms with optimal approximation properties for images with edges [2], [12].

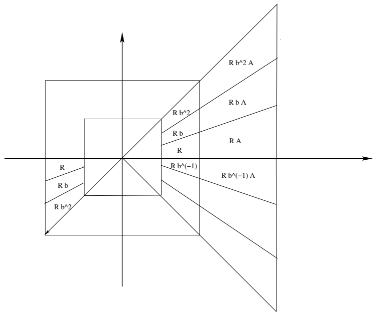

Fig. 4. *Example of composite wavelet system with $a = 2I$ and shearing matrix.*

III. Critically Sampled Transforms

We will now develop some examples of discrete critically sampled transforms whose spatial-frequency tilings is consistent with some of the constructions given above. In particular, we will take advantage of a critically sampled 2D separable discrete wavelet transform (DWT) and of the quincunx-based discrete wavelet transform (QDWT) in our constructions.

For brevity, we describe the construction using a critically sampled 2D separable DWT; the other case is similar. Given a one dimensional scaling function ϕ and a wavelet function ψ, the three functions $\psi^1(x) = \phi(x_1)\psi(x_2)$, $\psi^2(x) = \psi(x_1)\phi(x_2)$, and $\psi^3(x) = \psi(x_1)\psi(x_2)$ generate an orthogonal basis for $L^2(\mathbb{R}^2)$ by translation and dilation. Define $\psi^k_{j,n}(x) = 2^{j/2}\psi^k(2^j x - n)$ for $k = 1$ to 3 where j determines the scale and $n \in \mathbb{Z}^2$. These determine basis functions for the detail subspace $V_j \otimes W_j$, $W_j \otimes V_j$, and $W_j \otimes W_j$ where V_j and W_j denote the 1D approximation space and detail space determined by the 1D scaling and wavelet functions. The 2D approximation space is $V_j \otimes V_j$ and is generated by $\{2^{j/2}\phi^2(2^j x - n)\}_{n\in\mathbb{Z}^2}$ where $\phi^2(x) = \phi(x_1)\phi(x_2)$.

To construct our directional filters corresponding approximately to the construction of Example 3, we define

$$S^{(0)}(\omega) = S_1(\omega_1)S_2(\tfrac{\omega_2}{\omega_1}),\ S^{(1)}(\omega) = S_1(\omega_2)S_2(\tfrac{\omega_1}{\omega_2})$$

where S_1,$S_2 \in C^\infty(\mathbb{R})$ and are compactly supported. Under appropriate assumptions on S_1, S_2, we can choose $\Phi \in C_0^\infty(\mathbb{R}^2)$ to satisfy

$$|\Phi(\omega)|^2 + \sum_{d=0}^{1}\sum_{j\geq 0}\sum_{\ell=-2^j}^{2^j-1} |S^{(d)}(\omega a^{-j} b_d^{-\ell})|^2 \chi_{\mathcal{D}_d}(\xi) = 1$$

where $b_0 = \left(\begin{smallmatrix}1 & 1\\ 0 & 1\end{smallmatrix}\right)$, $b_1 = b^T$, $\omega \in \mathbb{R}^2$ and $\mathcal{D}_d$ is given in Example 3.

Define $\phi_k(x) = \phi(x-k)$, where $\phi = (\Phi)^\vee$, and $s^{(d)}_{j,\ell,k}(x) = 2^{\frac{3j}{2}}\, s^{(d)}(b_d^\ell a^j x - k)$, where $s^{(d)} = (S^{(d)})^\vee$. Then the collection of $\{\phi_k : k \in \mathbb{Z}^2\}$ together with

$$\{s^{(d)}_{j,\ell,k}(x) : j \geq 0,\ -2^j + 1 \leq \ell \leq 2^j - 2,\ k \in \mathbb{Z}^2, d = 0, 1\}$$

$$\cup\{\tilde{s}^{(d)}_{j,\ell,k}(x) : j \geq 0,\ \ell = -2^j, 2^j - 1,\ k \in \mathbb{Z}^2, d = 0, 1\},$$

is a Parseval frame for $L^2(\mathbb{R}^2)$, where $\tilde{S}^{(d)}_{j,\ell,k} = S^{(d)}_{j,\ell,k}\,\chi_{\mathcal{D}_d}$ (the last set is needed to take care of the corner elements).

We can now form a decomposition of the complement of the 2D approximation space at level j for a fixed j_0 with $k \in \mathbb{Z}^2$ $(d = 0, 1)$ to be

$$\sum_{k'} s^{(d)}_{j_0,\ell,k-k'}(x)\psi^1_{j,k}(x),\ \sum_{k'} s^{(d)}_{j_0,\ell,k-k'}(x)\psi^2_{j,k}(x),$$

$$\sum_{k'} s^{(d)}_{j_0,\ell,k-k'}(x)\psi^3_{j,k}(x)$$

with $-2_0^j + 1 \leq \ell \leq 2_0^j - 2$ and

$$\sum_{k'} \tilde{s}^{(d)}_{j_0,\ell,k-k'}(x)\psi^1_{j,k}(x),\ \sum_{k'} \tilde{s}^{(d)}_{j_0,\ell,k-k'}(x)\psi^2_{j,k}(x),$$

$$\sum_{k'} \tilde{s}^{(d)}_{j_0,\ell,k-k'}(x)\psi^3_{j,k}(x)$$

with $\ell = -2^j, 2^j - 1$. Since the transform based on this decomposition combines a discrete wavelet transform (DWT) and a component of the shearlet transform, it will be referred to as the *DWTShear* transform. The implementation is based on using a Meyer wavelet for the shearlet-based component [12], [13]. The analogous transform based on using the quincunx-based discrete wavelet transform (QDWT) will be referred to as *QDWTShear*. This produces a spatial-frequency tiling of a wavelet with composite dilations equivalent to Example 1. Further details on this implementation are described in [14]

Note that, in this decomposition, j_0 is constant so that an image coding scheme can take advantage of the correlation between levels in the DWT. In particular, one can benefit from tree-based coding schemes to improve this decay rate [15]. This is in contrast to similar schemes which do not fix the number of angular divisions in order to try and maintain a parabolic scaling law of $width \propto height^2$.

IV. Experimental Results

In this section, we present results of our proposed algorithms and compare their nonlinear approximation (NLA) capabilities to those of the full hybrid DWT (HDWT), the full hybrid QDWT (HQDWT) [8], the non-uniform directional filter based (NUDFB), the quincunx non-uniform directional filter based (QNUDFB) [16], and the critically sampled contourlet transform (CSCT) [3].

We used the images *Barbara*, *Einstein*, and *Elaine* shown in Figure 5. In our implementation of DWTShear and QDWTShear transforms we used a 4 level decomposition DWT with j_0 set to 6. Figure 6 illustrates a decomposition when j_0 is set to 3 for easy interpretation. An improved performance is possible by using a larger number of decomposition levels for the DWT but a 4 level decomposition of the DWT was used to have a transform comparable in decomposition to those used [8],[16], and [3].

V. Conclusion

In this paper, we have shown that the framework of wavelets with composite dilations provides a very flexible tool to generalize a number of oriented transforms recently appeared in the literature, and to construct new ones. Within this setting,

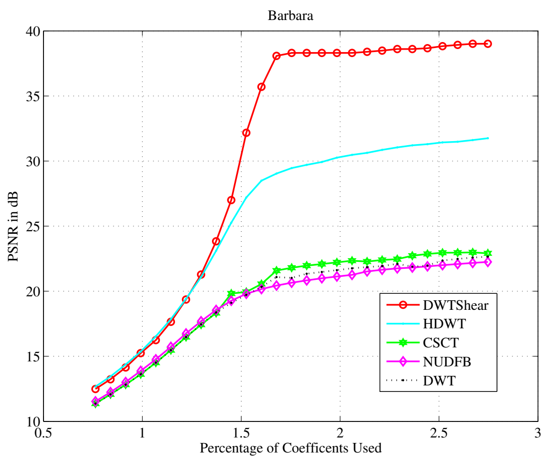

(a)

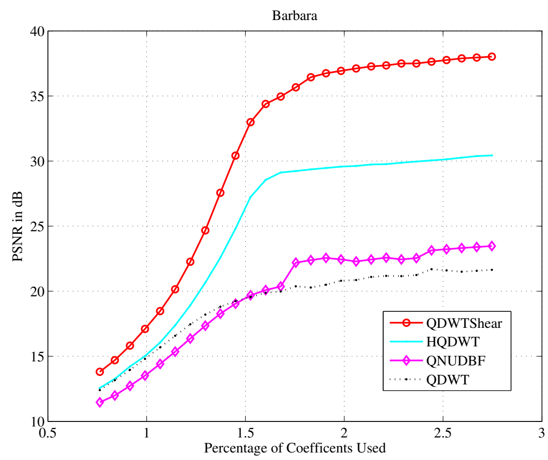

(b)

Fig. 7. .

(a)

(b)

(c)

(d)

(e)

(f)

Fig. 8. Details of the nonlinear approximations using 4150 coefficients with the *Einstein* image. (a) Original image. (b) DWTShear (PSNR=44.55 dB). (c) HQDWT (PSNR=34.79 dB). (d) HDWT (PSNR=32.54 dB). (e) QNUDFB (PSNR=26.85 dB). (f) NUDFB (PSNR=26.71 dB).

we derive a new critically sampled transform referred to as the DWTShear transform and its quincunx companion the QDWTShear transform. Various experiments demonstrate that these transforms can sparsely represent a wide class of images and achieve excellent nonlinear approximation capabilities. Such transforms can be applied to image coding very effectively.

References

[1] E. J. Candès and D. L. Donoho, "New tight frames of curvelets and optimal representations of objects with piecewise C^2 singularities," *Comm. Pure and Appl. Math.*, vol. 56, pp. 216–266, 2004.

[2] K. Guo and D. Labate, "Optimally sparse multidimensional representation using shearlets", *SIAM J. Math. Anal.*, vol. 9, pp. 298–318, 2007.

[3] S. Higaki, S. Kyochi, Y. Tanaka, and M. Ikehara, "A novel design of critically sampled contourlet transform and its application to image coding," *Proc. IEEE Int. Conf. Image Process. ICIP2008.* San Diego, CA, Oct. 2008.

[4] M. N. Do, and M. Vetterli, "The contourlet transform: an efficient directional multiresolution image representation", *IEEE Trans. Image Process.*, vol. 14, no. 12, pp. 2091-2106, Dec. 2005.

[5] D. D. Po and M. N. Do, "Directional multiscale modeling of images using the contourlet transform," *IEEE Trans. Image Process.*, vol. 15, pp. 1610–1620, 2006.

[6] R. Eslami, H. Radha, "New image transforms using hybrid wavelets and directional filter banks: Analysis and design," *Proc. IEEE Int. Conf.*

(a)

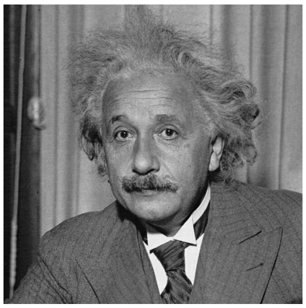

(b)

(c)

Fig. 5. Images used in this paper for different experiments. (a) *Barbara* image, (b) *Einstein* image, (c) *Elaine* image.

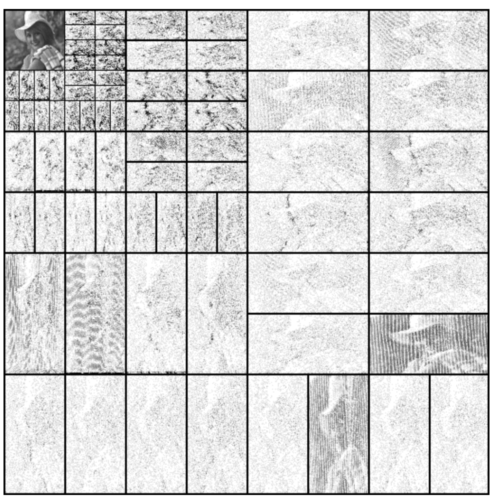

Fig. 6. Example images of the DWTShear decompositions of the *Elaine* image using 8 angular subdivisions in each quadrant and 4 scales.

TABLE I
PSNR VALUES OF THE NLA FOR THE BARBARA IMAGE.

Num. of coeff.	1050	1350	1600	1950	2250
DWTShear	35.70	38.31	38.67	39.18	39.62
HDWT	27.41	29.87	30.50	31.14	31.54
CSCT	20.55	22.35	22.86	23.02	24.08
NUDFB	20.16	21.26	21.91	22.50	23.42
DWT	20.34	21.76	21.98	22.90	23.50
QDWTShear	34.39	37.11	37.63	38.14	38.53
HQDWT	28.55	29.63	30.05	30.84	31.24
QNUDFB	20.08	22.29	23.14	23.77	23.91
QDWT	19.88	20.86	21.69	22.51	22.49

TABLE II
PSNR VALUES OF THE NLA FOR THE EINSTEIN IMAGE.

Num. of coeff.	4150	5400	6400	6900	7400
DWTShear	44.55	45.40	45.74	45.82	45.93
HDWT	32.54	33.79	34.47	34.72	34.98
CSCT	26.32	28.31	28.50	28.84	29.13
NUDFB	26.71	28.57	29.12	29.11	29.31
DWT	26.18	28.58	28.84	29.05	29.20
QDWTShear	39.70	43.75	44.17	44.32	44.54
HQDWT	34.79	36.12	36.70	36.87	37.05
QNUDFB	26.85	28.38	28.81	29.00	29.10
QDWT	26.10	27.58	27.63	27.75	27.90

TABLE III
PSNR VALUES OF THE NLA FOR THE ELAINE IMAGE.

Num. of coeff.	4150	5400	6400	6900	7400
DWTShear	45.98	47.05	48.03	48.46	48.80
HDWT	32.90	34.41	34.97	35.22	35.50
CSCT	27.46	29.34	30.00	30.31	30.43
NUDFB	28.31	30.38	30.82	31.00	31.01
DWT	27.86	29.98	30.91	31.08	31.34
QDWTShear	46.35	47.50	48.00	48.15	48.29
HQDWT	35.60	38.16	39.12	39.50	39.85
QNUDFB	28.02	30.05	30.72	31.06	31.24
QDWT	27.74	29.72	30.30	30.72	30.94

Image Process. ICIP2005. Genova, Italy, Sept. 2005.

[7] R. Eslami and H. Radha, “Regular hybrid wavelets and directional filter banks: Extensions and applications,” *Proc. IEEE Int. Conf. Image Process. ICIP2006.* Atlanta, GA, Oct. 2006.

[8] R. Eslami, H. Radha, “A New Family of Nonredundant Transforms Using Hybrid Wavelets and Directional Filter Banks,” *IEEE Trans. Image Process.* vol. 16, no. 4, pp. 1152–1167, 2007.

[9] K. Guo, W.-Q Lim, D. Labate, G. Weiss and E. Wilson, “Wavelets with composite dilations,” *Electron. Res. Announc. Amer. Math. Soc.*, vol. 10, pp. 78–87, 2004.

[10] K. Guo, W-Q. Lim, D. Labate, G. Weiss and E. Wilson, “Wavelets with composite dilations and their MRA properties,” *Appl. Comput. Harmon. Anal.* vol. 20, pp. 220–236, 2006.

[11] K. Guo, W-Q. Lim, D. Labate, G. Weiss and E. Wilson, “The theory of wavelets with composite dilations,” in: Harmonic Analysis and Applications, C. Heil (ed.), pp. 231–249, Birkhäuser, Boston, MA, 2006.

[12] G. Easley, W. Lim, and D. Labate, “Sparse Directional Image Representations using the Discrete Shearlet Transform,” *Appl. Comput. Harmon. Anal.,* vol. 25, pp. 25–46, 2008.

[13] W-Q. Lim, “Wavelets with Composite Dilations,” Ph.D. Thesis, Dept. Mathematics, Washington University in St. Louis, St. Louis, MO, 2006.

[14] G. Easley, and D. Labate, “Theory and Applications of Critically Sampled Composite Wavelets,” preprint.

[15] A. Cohen, I. Daubechies, O. Guleryuz, and M. Orchard, “On the importance of combining wavelet-based non-linear approximation with coding strategies,” *IEEE Trans. Inf. Theory*, vol. 48, no. 7, pp. 1895-1921, Jul. 2002.

[16] T. T. Nguyen and S. Oraintara, “Multiresolution direction filterbanks: Theory, design, and applications,” *IEEE Trans. Signal Process.*, vol. 53, no. 10, pp. 3895-3905, Oct. 2005.